Chapter 5
Adsorbed nanoparticles on bipolar droplets

The results presented in this chapter are to be submitted as a paper to **Soft Matter** under the title *"Topological dereliction in liquid crystal mediated nano-particle assembly on spherical droplets"*.

Nanoparticles embedded in liquid crystalline surfaces offer novel platforms for sensing and material design. These systems rely on the nematic mediated driven assembly that generates an interesting portfolio of patterns and geometric arrangements that provide extraordinary optical properties [192]. Pure spherical nematic LC droplets adopt radial or bipolar phases depending on the anchoring orientation at the surface, *i.e.*homeotropic or planar respectively. A bipolar droplet align the molecules along the surface forming two "boojum" defects at two opposite poles. On the other hand, a radial droplet, where the preferred alignment at the surface is perpendicular, shows a point defect at the droplet center. As nano-particles are included in any nematic field, systems undergo a set of energy penalizations that drive the organization of the particles in specific arrangements in search for annihilation of high-splay regions [193–196].

In bipolar droplets, where the defect structures or boojums are close to the surface, energy minimization mediates the assembly of particles at the droplet surface. Experimentally it has been observed that once fluorescent polystyrene (PS) nanoparticles are adsorbed onto an LC bipolar droplet, there is a preference to locate at the poles [37]. Previous research done with molecular and continuum simulations show a comprehensive view of how the balance between bulk and surface distortions aims to annihilate defects, ultimately determining the assembly of systems with

up to three nanoparticles [44, 43, 197]. This phenomenon is analog to self assembly processed in biological systems [198, 199].

As the number of particles increases, the possible arrays of the nanoparticles follow permutation rules with probabilities associated with local minima free energy. We found that final particle assembly is controlled by a combination of the detailed balance between bulk and surface distortions, a general mechanism to minimize the presence of defects, and the available space to accommodate particles on the surface. As the number of particles increases, conventional approaches fail to cover the whole spectrum of configurations adopted by the particles. The varied topology of the assemblies alters the free energy landscape, so the resulting configuration is not necessarily the most compact or efficient arrangement, instead systems are trapped in near-global minima that features variations on the geometry of the patterns. The underlying feature of this ordering mechanism is topological dereliction, similar to any glass forming system where the multitude of diverging pathways open the way to otherwise unstable arrays [200, 201].

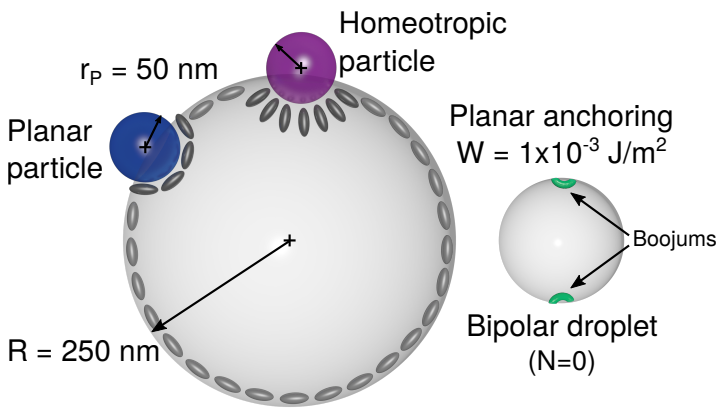

Figure 5.1. Schematic of planar (blue) and homeotropic (purple) particles with radius r_P half-submerged in a planar droplet with radius R. Strong anchoring conditions induce a bipolar configuration in the droplet, when no particles are present, characterized by two boojums (green) in opposite poles.

In this letter, we aim to describe the underlying physics that drive particle localizations by studying bipolar LC droplets containing up to ten half-submerged nano-particles, homeotropic and planar, on the surface as illustrated in figure 5.1. We developed a novel Monte Carlo (MC) sampling algorithm that allows particles to be moved and sample freely during the free energy minimization. With this approach, particle location does not require to be fixed and multi-particle ordering is

actually an additional result. The method adopts Metropolis sampling criteria for the alignment tensor [61] and the particle position. When particles move, a localized Ginzburg-Landau (GL) minimization is used to relax the alignment tensor in the neighborhood of the previous and current particle location. Every final particle configuration predicted by the MC was also minimized by a global GL to validate energy minima values.

Every final particle configuration predicted by the MC was also minimized by a global GL to validate energy minima values. The results show that, as the number of particles is increased, a topological entropy, given by the spherical confinement and the reduced space to locate particles, plays an important role in the final particle assembly. Its effects are so important, that drops with four and five nano-particles the global minima is never observed, and the systems are trapped in a local minima that mimics the three nanoparticle system. On the other hand, for more than six particles global and near-global minima are observed, which exhibited an ample variety of geometric variations of the assemblies. The possible combinations and geometric arrays for more than 8 particles make for an extremely extensive study. Here, we report on configurations found by starting from different random seeds, but not enough to cover and found all possible combinations.

The LC is described in terms of the local alignment tensor $\mathbf{Q}(\mathbf{x})$, which is defined in terms of the second moment of the molecular orientational distribution function, $\psi(\mathbf{u},\mathbf{x},t)$, $\mathbf{Q}(\mathbf{x}) = \int(\mathbf{uu} - \frac{\boldsymbol{\delta}}{3})\psi(\mathbf{u},\mathbf{x},t)d\mathbf{u}$, where $\mathbf{u}(\mathbf{x})$ is the ensemble average of molecular orientations. At each configuration of the alignment tensor field $\mathbf{Q}(\mathbf{x})$ is assigned a probability proportional to the Boltzmann factor $\exp\left[-\beta F(\mathbf{Q}(\mathbf{x}))\right]$, where $\beta^{-1} = k_B\hat{T}$, k_B is the Boltzmann constant and $\hat{T}$ is the fluctuating temperature. The coarse-grained free energy functional (or Hamiltonian) is taken as the sum of three terms: a short-range Landau polynomial expansion in $\mathbf{Q}(\mathbf{x})$ −to describe the isotropic-nematic (IN) transition−, a long-range free energy density −for elastic distortions− and a surface free energy contribution:

$$F(\mathbf{Q}) = \int d^3\mathbf{x}\left[f_L(A,U,\mathbf{Q}) + f_E(L_1,\nabla\mathbf{Q})\right] + \oint d^2\mathbf{x} f_S(W,\mathbf{Q}), \tag{5.1}$$

where A sets the energy density scale for the model, dimensionless parameter U determines the IN transition, L_1 is an elastic constant and W represents the strength of the surface anchoring.

The free energy densities are described in detail in section 2.1.2. The LC parameters define two characteristic length scales: the nematic coherence length $\xi_N = \sqrt{L_1/A}$ and the surface extrapolation length $\xi_S = L_1/W$.

A Monte Carlo (MC) scheme is used to generate a Markov chain of states. Random updates to the alignment tensor field or the particle positions, are proposed and accepted according to a Metropolis criteria, which ensures the detailed balance. We generate a new configuration "n" from an old configuration "o" with a probability $P_{\text{prop}}(o \to n)$, which is accepted according to the criterion:

$$P_{\text{acc}}(o \to n) = \min\left[1, \exp(-\beta \Delta F)\right], \tag{5.2}$$

where $\Delta F = F(\mathbf{Q}(n)) - F(\mathbf{Q}(o))$ is the energy difference between the new and the old configuration. When the alignment tensor is changed at a point $\mathbf{x}_\nu$, numerical approximation is used to calculate $\mathbf{Q}(\mathbf{x}_\nu)$, $\nabla\mathbf{Q}(\mathbf{x}_\nu)$ and $F(\mathbf{Q}(\mathbf{x}_\nu))$. On the other hand, when the position of a particle $\mathbf{x_p}$ is changed, localized Ginzburg-Landau (GL) relaxations are done in the neighborhood of the new and old particle position; in the latter LC fills the empty space with random orientations. After a short GL, over several relaxation times, the "new" state is defined and the Hamiltonian is integrated numerically. The GL evolution towards equilibrium is explained in section 2.3.1.

The trick for the MC is to be able to sample all possible configurations from Markov displacements of $\mathbf{Q}$'s proper values. We start by recognizing that $\mathbf{Q} = S\left[\mathbf{nn} - \delta/3\right] + \eta\left[\mathbf{n'n'} - (\mathbf{n}\times\mathbf{n'})(\mathbf{n}\times\mathbf{n'})\right]$, where $S(\mathbf{x})$ is the scalar order parameter, related to the maximum eigenvalue $2S/3$, and $\eta(\mathbf{x})$ is the biaxiality, related to the other two eigenvalues $\pm\eta - S/3$. In addition, S and η are bounded by $S \in [-\frac{1}{2}, 1]$ and $\eta \in [-\frac{1}{3}(1-S), +\frac{1}{3}(1-S)]$. The eigenvectors, $\mathbf{n}$ and $\mathbf{n'}$, related to the maximum and second largest eigenvalues, define an orthonormal basis $\{\mathbf{n}, \mathbf{n'}, (\mathbf{n}\times\mathbf{n'})\}$ for the LC orientations. Therefore, attempting Markov chains for S, η, $\mathbf{n}$ or $\mathbf{n'}$ would require cumbersome schemes that may break the detailed balance. Now, the alignment tensor is symmetric and traceless, and out of its nine cartesian components only five are actual degrees of freedom. Thus, it can be expressed in terms of an orthonormal tensor basis [93, 202, 203]:

$$\mathbf{Q}\left(\mathbf{x}, t\right) = \sum_{\nu}^{5} a_\nu\left(\mathbf{x}, t\right)\mathbf{T}^\nu, \tag{5.3}$$

where the orthonormal basis is defined by five tensors:

$$\begin{aligned}
\mathbf{T}^1 &= \sqrt{3/2}\,[\mathbf{zz}]^{\mathsf{ST}} = \sqrt{3/2}\,(\delta_{33} - \delta_{ij}/3)\,, \\
\mathbf{T}^2 &= \sqrt{2}\,[\mathbf{xy}]^{\mathsf{ST}} = \sqrt{2}\,(\delta_{1i}\delta_{2j} + \delta_{2i}\delta_{1j})\,/2, \\
\mathbf{T}^3 &= \sqrt{2}\,[\mathbf{xz}]^{\mathsf{ST}} = \sqrt{2}\,(\delta_{1i}\delta_{3j} + \delta_{3i}\delta_{1j})\,/2, \\
\mathbf{T}^4 &= \sqrt{1/2}\,(\mathbf{xx} - \mathbf{yy}) = \sqrt{1/2}\,(\delta_{1i}\delta_{1j} - \delta_{2i}\delta_{2j})\,, \\
\mathbf{T}^5 &= \sqrt{2}\,[\mathbf{yz}]^{\mathsf{ST}} = \sqrt{2}\,(\delta_{2i}\delta_{3j} + \delta_{3i}\delta_{2j})\,/2,
\end{aligned} \tag{5.4}$$

where $\mathbf{x}$, $\mathbf{y}$ and $\mathbf{z}$ are the canonic $\Re^3$ basis and δ_{ij} is the Kronecker delta. Because the $\{\mathbf{T}^m\}$ basis is orthonormal $\mathrm{tr}(\mathbf{T}^m\mathbf{T}^n) = T^m_{ij}T^n_{ij} = \delta_{mn}$, it ensures that the five scalar components a_ν of the alignment tensor are simple projections: $a_\nu = \mathrm{tr}(\mathbf{Q}\mathbf{T}^\nu)$; the $\mathbf{a}$ set provides a unique and independent way to specify a particular configuration of the alignment tensor field.

5.1 Description of the MC method

In this work we implement a novel MC theoretically informed method [60, 61] to study the directed self-assembly of nanoparticles on the surface of LC bipolar droplet. This new tool allows to obtain self-organized assemblies of colloidal particles at the nanoscale level.

The methodology utilized here is based mainly on the work previously reported by Armas-Pérez [60, 61] where a Metropolis MC scheme was applied to minimize the free energy functional making trial random updates of the alignment tensor field to reach the equilibrium states. As an extension, trial Monte Carlo displacements of nanoparticles are proposed. This new implementation allows to explore the formation of organized assemblies of colloids on the surface of LC droplet.

The free energy associated to LC bulk was reached utilizing a stochastic sampling method. The field is approximated on a discrete mesh setting N collocation points. A collocation point is selected randomly, in the bulk or surface, and a MC trial move is attempted by randomly displacing $\mathbf{a}(\mathbf{x})$ according to [60] $a_{\mu,n}(\mathbf{x}) = a_{\mu,o}(\mathbf{x}) + \bar{\delta_\mu}(\lambda - 0.5)$ where "n" and "o" indicate the new and old trial configurations, respectively. μ is chosen in random way from 1 to 5 and λ is a random number distributed uniformly between $[0, 1]$. $\bar{\delta_\mu}$ is the maximum allowed displacement of a_μ and it is

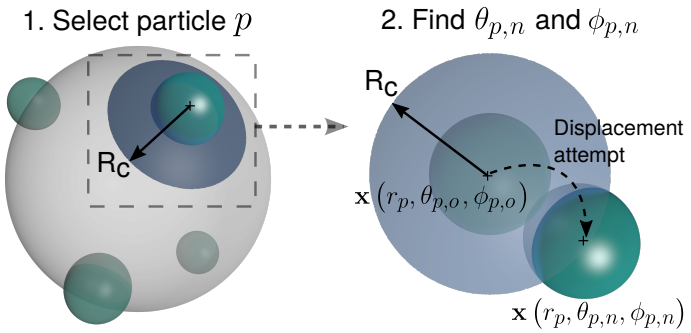

Figure 5.2. Schematic of displacement attempt for nanoparticles on the droplet surface.

adjusted periodically during the minimization to achieve an average 30% acceptance rate. For each MC move, the physical bounds for the tensor $\mathbf{Q}$ are always enforced.

For the nanoparticles location, we proposed two types of advance sampling techniques: the first one is to try a MC move sampling positions within a "surface circle" that in spherical coordinates does not exceed θ or ϕ by more than 0.1π. In this case, a particle located at position $\mathbf{x}(r_p, \theta_p, \phi_p)$ (in spherical coordinates) is selected randomly and its displacement is attempted by following,

$$\begin{aligned} \theta_{p,n} &= \theta_{p,o} + \delta_\theta(\xi_1 - 0.5), \\ \phi_{p,n} &= \phi_{p,o} + \delta_\phi(\xi_2 - 0.5), \end{aligned} \tag{5.5}$$

where "n" and "o" indicate the new and old trial configurations, respectively; p is chosen in a random way from 1 to N (being N the total number of nanoparticles), and ξ_1 and ξ_2 are random numbers distributed uniformly between $[0, 1]$. δ_θ and δ_ϕ are the maximum allowed displacement of θ and ϕ and they are fixed to value $\delta_\theta \approx 0.11\pi$ and $\delta_\phi \approx 0.11\pi$. The second displacement was implemented in order to test positions far away from it, reaching configurations that otherwise would be very difficult to get in. For this case, the whole domains $\theta \in [0, \pi]$ and $\phi \in [0, 2\pi]$ are explored. The new position is obtained randomly from θ and ϕ domains according to:

$$\theta_{p,n} = \pi\xi_1, \quad \phi_{p,n} = 2\pi\xi_2 \tag{5.6}$$

ξ_1 and ξ_2 are random numbers distributed uniformly between $[0, 1]$. r_p is always enforced equal to 1. For each move, we avoid overlapping between particles.

Two crucial issues must be taken into account to generate a trial configuration. One is to fill in the empty space on the site that the colloid left; the second one is to make a suitable tensor field surrounding the nanoparticle at the new site. We proposed to avoid the first issue filling the empty space with a field obtained from an average tensor. As a second step, we proposed to applied a traditional Ginzburg-Landau relaxation to get desirable tensor fields on both sites. We determined that the relaxation will be applied only for collocation points whom are inside a sphere with a cut off radius R_c. We found heuristically that $R_c = 1.5r_P$ (r_P is the particle radius) is enough to create an acceptable configuration. The main advantage to apply this implementation is that the acceptance rate is around 30%-5%, depending of the effective temperature $\hat{T}$. We have attempted to create between 100,000 and 400,000 accepted MC moves per particle.

5.2 Results

An LC droplet with radius $R = 250$ nm with half-submerged nano-particles with radius $r_P = 0.2R = 50$ nm are considered. 4'-pentyl-4-cyanobiphenyl (5CB) was used as the model system for the LC: $A \approx 1 \times 10^5$ J/m^3 and $L_1 = 5.11$ pN and $\xi_N = 7.15$ nm. The LC droplet follows a strong degenerate planar anchoring with strength $W = 1 \times 10^{-3}$ J/m^2, which induces a bipolar configuration characterized by two boojum defects at opposite poles. In the Landau-de Gennes framework, bulk systems are expected to be in the isotropic phase for values of $U < {}^{8}/_{3}$, and in the nematic phase for $U \geq 2.8$. For results showed here, we have adopted $U = 5$ corresponding to a bulk scalar order parameter $S \approx 0.76$. A finite differences scheme is used to approximate fields and gradients, where spheres of sizes R and r_P are embedded in cubes of uniform meshes. The mesh resolution was selected in such a way that length scales are resolved appropriately. Typical meshes used between 1 and 2 million nodes. MC relaxations where done by an exponential temperature annealing until 500,000 to 1,000,000 accepted MC steps per node were reached. Study cases of nano-particles are divided into two categories. First, we simulated homogeneous sets of colloids, where all particles induce either perpendicular or parallel alignment of the LC molecules neighboring its surface. Then, heterogeneous sets are considered where we start with $N = 4$ with a number ratio of homeotropic particles (N_{H}) to planar particles (N_{P}) of 2:2 and gradually increase the number of particles by one of each type until $N = 10$ and $N_{\mathsf{H}} : N_{\mathsf{P}}$ of 5:5; this is done for

strong and moderate anchoring conditions at the particles surface. Finally, we study the case of a fixed number of particles ($N = 10$) and varying the number ratio $N_{\mathsf{H}} : N_{\mathsf{P}}$, with a moderate anchoring strength ($W = 1 \times 10^{-4}$ J/m^2). Simulations for each set of N particles started from 20 random configurations and different assemblies were found, suggesting the probabilistic nature of self-assembly.

5.2.1 Homeotropic particles

Based on previous studies [43, 44, 37], homeotropic particles with infinite anchoring are studied starting with $N = 2$ as shown in figure 5.3. As expected, the nanoparticles end up at the same location where boojums would be. This indicates that free energy is minimized by eliminating regions of high splay. The perpendicular orientation of LC molecules near the particle surface matches the inherent alignment of a bipolar droplet near the boojums, so no additional strain is generated in the system. This is evident for $N = 2$ where particles are in opposite poles and there are no abrupt changes of the director field.

We observe that for $N \leq 5$ all configurations are non-degenerate, meaning that simulations starting from different random configurations consistently yield the same final state with standard deviations of the free energy smaller than $1 \times 10^{-7} k_B T/\text{nm}^3$. In this cases, particles show a tendency to aggregate at one of the poles and generate a new defect structure, shown in green in figure 5.3. When two homeotropic particles encounter, half saturn ring forms between them, as seen for $N = 3$ and in insert (a). As more particles aggregate, the defect takes the shape of the junctures and fills the empty spaces between them. Degenerate states are observed for cases with $N > 5$, depicted in figure 5.3 as small round markers, exhibiting different ways of arranging the set of size N. For all cases, the state with maximum free energy is that with one particle in one boojum and $N - 1$ particles in the opposite side of the droplet that assemble in hexagonal, triangular or diamond-shape structures as labelled and drawn in the inserts. For the states of minimum free energy, particles tend to arrange more equitably with more than 2 particles in each pole, which is in agreement with experimental results reported by Wang *et al.* [37].